J|A|C|S

A Half-Zippered SNARE Complex Represents a Functional Intermediate in Membrane Fusion

Feng Li,*[†,⊥] Daniel Kümmel,[†,⊥,§] Jeff Coleman,[†,⊥] Karin M. Reinisch,[†,⊥] James E. Rothman,[†,⊥] and Frederic Pincet*[†,⊥,‡]

[†]Department of Cell Biology, School of Medicine, Yale University, 333 Cedar Street, New Haven, Connecticut 06520, United States
[⊥]Nanobiology Institute, Yale University, West Haven, Connecticut 06516, United States
[‡]Laboratoire de Physique Statistique, UMR CNRS 8550 Associée aux Universités Paris 6 et Paris 7, Ecole Normale Supérieure, 24 Rue Lhomond, 75005 Paris, France

S *Supporting Information*

ABSTRACT: SNARE (soluble *N*-ethylmaleimide-sensitive factor attachment protein receptor) proteins mediate fusion by pulling biological membranes together via a zippering mechanism. Recent biophysical studies have shown that t- and v-SNAREs can assemble in multiple stages from the N-termini toward the C-termini. Here we show that functionally, membrane fusion requires a sequential, two-step folding pathway and assign specific and distinct functions for each step. First, the N-terminal domain (NTD) of the v-SNARE docks to the t-SNARE, which leads to a conformational rearrangement into an activated half-zippered SNARE complex. This partially assembled SNARE complex locks the C-terminal (CTD) portion of the t-SNARE into the same structure as in the postfusion 4-helix bundle, thereby creating the binding site for the CTD of the v-SNARE and enabling fusion. Then zippering of the remaining CTD, the membrane-proximal linker (LD), and transmembrane (TMD) domains is required and sufficient to trigger fusion. This intrinsic property of the SNAREs fits well with the action of physiologically vital regulators such as complexin. We also report that NTD assembly is the rate-limiting step. Our findings provide a refined framework for delineating the molecular mechanism of SNARE-mediated membrane fusion and action of regulatory proteins.
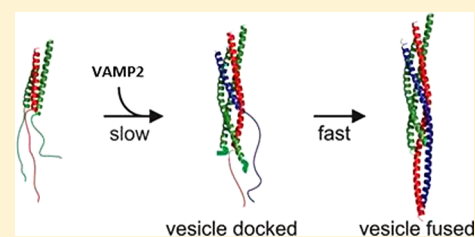
INTRODUCTION

The essential and highly conserved SNARE (soluble *N*-ethylmaleimide-sensitive factor attachment protein receptor) proteins are the molecular machines that drive membrane fusion, which represents the final step in every trafficking pathway.[1−4] The neuronal SNARE complex, consisting of VAMP2 bound to the synaptic vesicle (v-SNARE) and syntaxin1A and SNAP25 on the target membrane (t-SNARE), has been extensively studied and serves as a model system for understanding complex assembly and SNARE-mediated membrane fusion.[5,6] SNARE proteins are characterized by the presence of the heptad repeat motif that consists of mostly hydrophobic "layer residues" at every third or fourth position (layers numbered −7 to +8, Figure 1A).[7−9] Isolated SNAREs are largely unstructured but adopt an α-helical conformation upon interaction with their cognate binding partners.[10,11] A progressive zippering model was proposed for SNARE assembly, which suggests that the SNARE motifs from VAMP2, syntaxin1A and SNAP25, zipper directionally from their membrane-distal N-terminal domains (NTDs) to their C-terminal domains (CTDs) into a four-helical coiled-coil bundle.[8,12−15] Interactions extend through the membrane-proximal linker domains (LDs) and the transmembrane domains (TMDs) helices of SNAREs. The energy from complex formation is thought to be used to overcome the thermodynamic barrier of membrane fusion.[15,16] The zippering reaction has been historically considered to take place continuously as a single event,[8,12−15,17] but recent biophysical studies are more consistent with the idea that it occurs in discrete steps.[18−23] However, the functional significance of these biophysical observations has not been tested, which is our goal here.

Neuronal SNARE assembly is positively regulated by the SM protein Munc18[24−26] and controlled by a "clamping" system consisting of complexin and synaptotagmin for Ca^{2+}-dependent rapid and synchronized fusion.[27−34] It is not known how all these regulatory proteins interact with SNAREs on a molecular level. The hypothesis we will explore here is that a partially assembled SNARE complex represents a folding intermediate on which regulators might act to accelerate or decelerate SNARE assembly.

Here we demonstrate for the first time that even in the absence of any regulatory protein, a half-zippered SNARE complex represents a functional intermediate in a two-step folding process, and this intrinsic property of SNAREs provides a molecular basis that supports the models put forward for the function of complexin.[34] We show distinct functions for N- and
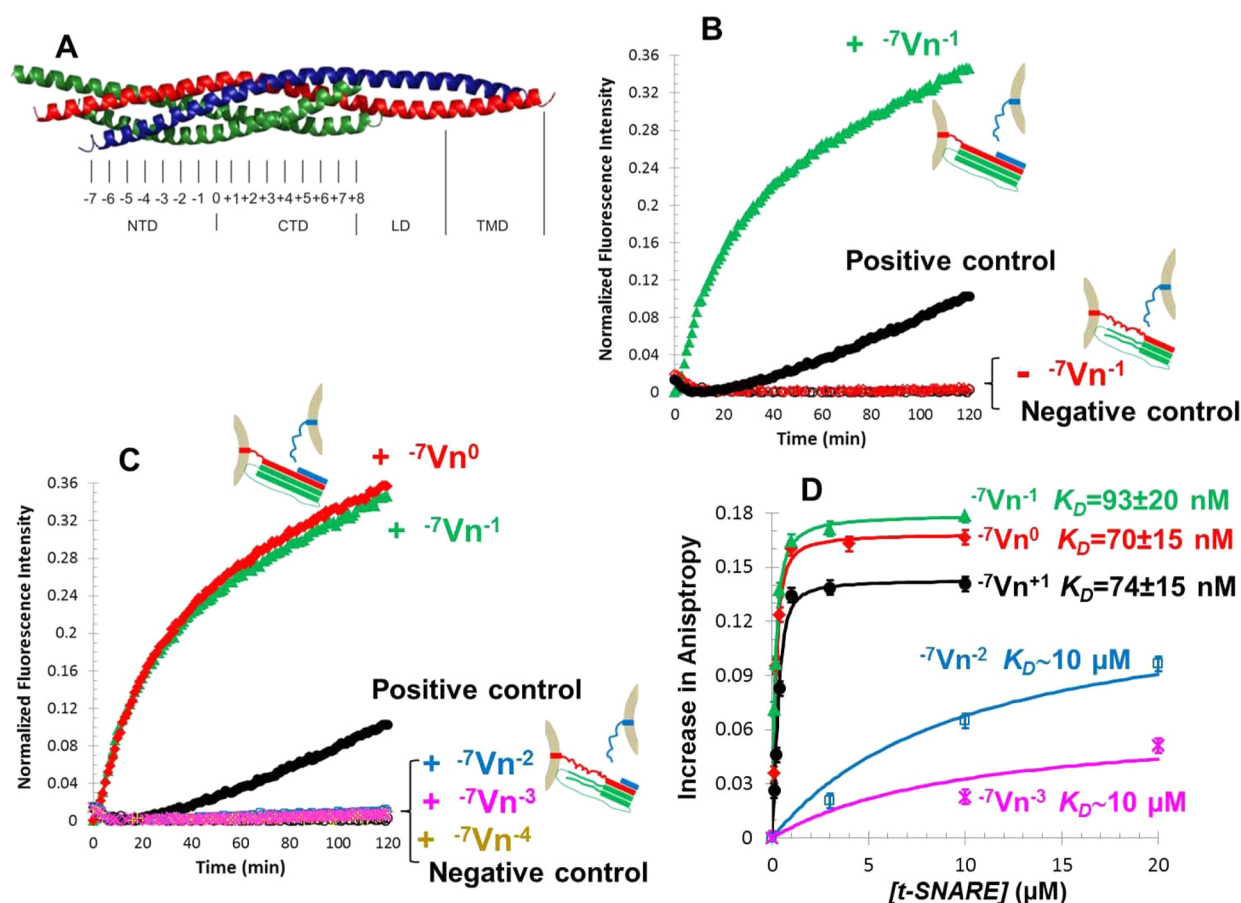
Figure 1. A switch that activates the t-SNARE exists in NTD assembly of SNARE complex. (A) Illustration of 4 domains and 16 layers in postfusion SNARE complex. The SNARE motifs form a four-helix bundle (syntaxin 1A, red; SNAP25, green; VAMP2, blue). (B) Vn peptide activates fusion between FLT-liposomes and Vc-liposomes. Standard liposome fusion assays were performed in the absence and presence of prebound $^{-7}Vn^{-1}$ (VAMP2 residues from layers -7 to -1) peptide. To prebind the Vn peptide, FLT-liposomes and $\sim 20\ \mu M\ ^{-7}Vn^{-1}$ peptide were incubated together at 37 °C for 60 min prior to mixing with Vc-liposomes. Positive control represents fusion of FLT-liposomes (full length t-SNARE) and FLV-liposomes (full length VAMP2), and negative control shows fusion of FLT-liposomes preincubated with CDV (the cytosolic domain of VAMP2, residues 1−94) and FLV-liposomes. (C) Activation of the t-SNARE requires SNAREs to assemble at least to layer -1. Fusion reactions were performed between $^{+1}Vc^{END}$-liposomes and FLT-liposomes prebound with $^{-7}Vn^{0}$, $^{-7}Vn^{-1}$, $^{-7}Vn^{-2}$, $^{-7}Vn^{-3}$, or $^{-7}Vn^{-4}$, respectively. Final concentrations of Vn peptides were $\sim 20\ \mu M$. (D) Layer -1 is required for Vn to bind tightly with the t-SNARE. Each individually labeled Vn (~ 200 nM) was incubated with cytosolic t-SNARE at various concentrations at 37 °C for 60 min followed by 24 h on ice. Fluorescence anisotropies of the resulting mixtures were measured. For each Vn, the increase in anisotropy was plotted versus t-SNARE concentration and fitted using eq 9 in Experimental Section to obtain the affinity constants.

C-terminal SNARE zippering, namely, prestructuring the t-SNARE and driving fusion, respectively.

■ EXPERIMENTAL SECTION

Protein Constructs, Expression, and Purification. The abbreviations of constructs used in this study are summarized in Supporting Table S1.

Full Length t-SNARE Complex (FLT). The full length t-SNARE complex, which includes full length, wild-type mouse His6-SNAP25 and rat Syn1A, was produced by expression of the polycistronic plasmid pTW34 in the BL-21 gold (DE3) *Escherichia coli* bacterial strain and purified as described before.[13,35−37]

Full Length VAMP2 (FLV). The full length VAMP2, which includes full length, wild-type mouse VAMP2, was produced by expression of the plasmid pTW2 in the BL-21 gold (DE3) *Escherichia coli* bacterial strain and purified as described before.[4,36,37]

Cytosolic t-SNARE Complex (CDT). The soluble t-SNARE complex, made of the cytoplasmic domain of rat syntaxin 1A (residues 1−265) and mouse His6-SNAP25 (residues 1−206), was produced by coexpression of pJM57 and pJM72 plasmids in the BL-21 gold (DE3) *Escherichia coli* bacterial strain and purified as described

before.[15,23,37] The protein concentration was typically 5−10 mg·mL^{-1} as determined by Bradford protein assay with BSA as the standard.

Cytosolic VAMP2 (CDV). The cytoplasmic domain of mouse His6-VAMP2 (residues 1−94, for fusion assay) and His6-SUMO-VAMP2 (residues 28−94, for circular dichroism assay) were produced by expression in the BL-21 gold (DE3) *Escherichia coli* bacterial strain and purified as previously described.[15,23,37] His6-SUMO tag was cleaved by SUMO protease. The protein concentration was typically 1.5−3 mg·mL^{-1} as determined by Bradford protein assay with BSA as the standard.

N-Terminal Domain of VAMP2 (Vn). The plasmids for the Vn variants were produced by cloning the N-terminus of VAMP2 of various lengths into a pCDFDuet-1 vector containing GST-PreScission-Vn (containing mouse VAMP2 N-terminal residues). The Vn constructs generated were $^{-7}Vn^{+1}$ (VAMP2 residues 28−60), $^{-7}Vn^{0}$ (VAMP2 residues 28−57), $^{-7}Vn^{-1}$ (VAMP2 residues 28−55), $^{-7}Vn^{-2}$ (VAMP2 residues 28−50), $^{-7}Vn^{-3}$ (VAMP2 residues 28−47), and $^{-7}Vn^{-4}$ (VAMP2 residues 28−44). These constructs were used in liposome−liposome fusion assay and circular dichroism experiments.

C-Terminal Domain of VAMP2 with Transmembrane Domain (TM-Vc). The plasmids for the TM-Vc variants were produced by cloning the C-terminus of VAMP2 of various lengths into a pET

SUMO vector containing N-terminal His$_6$ tag. The TM-Vc constructs generated were $^{-2}$Vc^{END} (VAMP2 residues 49−116), ^{0}Vc^{END} (VAMP2 residues 55−116), $^{+1}$Vc^{END} (VAMP2 residues 60−116), $^{+2}$Vc^{END} (VAMP2 residues 62−116), $^{+3}$Vc^{END} (VAMP2 residues 65−116), $^{+4}$Vc^{END} (VAMP2 residues 69−116), $^{+7}$Vc^{END} (VAMP2 residues 79−116), and ^{LD}Vc^{END} (VAMP2 residues 85−116).

All TM-Vc variants were expressed in BL21 gold (DE3) *Escherichia coli* bacterial strain. Cells were pelleted, resuspended, and passed through a cell disruptor. The lysate was centrifuged, and the supernatant was incubated with nickel-NTA beads. The beads were collected and washed. The His$_6$-SUMO tag was cleaved by incubating the protein (attached to nickel-NTA beads) with SUMO protease. The protein was eluted with a buffer containing 25 mM HEPES (pH 7.4), 400 mM KCl, 10% glycerol, 1 mM DTT, and 1% (w/v) *n*-octyl-β-D-glucopyranoside (OG).

SNARE-Liposome Reconstitution. The full length t-SNARE complex was reconstituted with the acceptor lipid mix made of 85 mol % POPC and 15 mol % DOPS. Full length VAMP2 and TM-Vc were reconstituted with the donor lipid mix comprising 82 mol % POPC, 15 mol % DOPS, 1.5 mol % DPPE-RHO, and 1.5 mol % DPPE-NBD.

The SNARE-liposome was prepared using the standard detergent removal method, which was previously reported.[4,13,35,36] Typically, FLT-liposome had 400:1 lipid/protein ratio and the FLV-liposome and Vc-liposome had 200:1 lipid/protein ratio.

Lipid-Mixing Fusion Assay. For a typical liposome−liposome fusion assay, 45 μL of FLT-liposome was mixed with 15 μL of buffer or Vn peptide (final concentrations of lipids and Vn peptide were ∼2 mM and ∼20 μM, respectively) and incubated at 37 °C for 60 min, then transferred to a 96-well FluoroNunc plates (Nalge Nunc, Rochester, NY) and kept at 37 °C for 5 min. The fusion reaction was initiated by adding 5 μL of Vc-liposome or FLV-liposome. Fusion between FLT-liposome and Vc-liposome was measured by monitoring the dequenching of the DPPE-NBD fluorescence resulting from its dilution into the fused liposomes, at 1 min intervals for 120 min, with excitation wavelength at 460 nm and emission wavelength at 538 nm, by a plate reader (Synergy H1 hybrid microplate reader, Bio-Tek). After 120 min, 10 μL of 2.5% (w/v) *n*-dodecylmaltoside (Boehringer, Ingelheim, Germany) was added to completely dissolve the liposomes. Measurement of the DPPE-NBD fluorescence was continued for another 40 min to obtain the DPPE-NBD fluorescence at infinite dilution. As reported previously,[4] the normalized fluorescence was obtained by using the fluorescence intensity of DPPE-NBD during fusion divided by the average intensity the DPPE-NBD fluorescence at infinite dilution.

Fluorescence Anisotropy. The Vn-S28C variants and cytosolic $^{+1}$Vc^{LD}-Cys (contains VAMP2 residues 58−94 and a single cysteine at the end of sequence) were labeled with Texas Red C2 maleimide (Invitrogen) according the protocol recommended by the manufacturer.

Fluorescence anisotropy was measured using the PC1 photon counting spectrofluorimeter (ISS). T-format polarization was used with a 625 nm long-path filter on the left-emission channel and a monochromator on the right-emission channel. The temperature of sample chamber was controlled with ±0.1 °C accuracy. For Texas Red labeled protein, the excitation wavelength was 580 nm and the emission wavelength at the right-emission channel was 612 nm. Quartz cuvette (Hellma) was used for all experiments.

For steady-state anisotropy measurements, the anisotropy of various Texas Red labeled Vn-S28C peptides was first measured in the absence of t-SNARE. Cytosolic t-SNARE (CDT) of various concentrations was then added to each labeled Vn peptide (∼200 nM). The mixtures were incubated at 37 °C for 60 min, followed by 24 h on ice. The anisotropy of each mixture was then respectively measured.

For kinetic studies, the Texas Red labeled cytosolic $^{+1}$Vc^{LD} peptide (72 nM) solution was introduced to a quartz cuvette (Hellma) with continuous and rapid magnetic stirring. Anisotropy was recorded as a function of time. Cytosolic t-SNARE prebound with Vn peptide or t-SNARE alone, at various concentrations, was injected into the cuvette and mixed rapidly. The data were plotted as anisotropy versus time, and the beginning of mixing was set as time zero.

To obtain the kinetics and thermodynamics parameters, we consider the following binding reaction:

$$V + T \leftrightharpoons VT$$
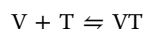
The kinetics equation is

$$\frac{d[VT]}{dt} = k_{on}[V][T] - k_{off}[VT] \tag{1}$$

where k_{on} is the on-rate, k_{off} is the off-rate, and [V], [T], and [VT] are the concentrations of VAMP2 peptide, t-SNARE, and SNARE complex at time t, respectively.

Let V_0 and T_0 be the initial concentration (or total concentration) of VAMP2 peptide and t-SNARE, respectively. Then

$$V_0 = [V] + [VT]$$

$$T_0 = [T] + [VT]$$

The measured anisotropy A at time t is an average of anisotropy of the fluorophores associated with VAMP2 peptide and the fluorophores associated with the SNARE complex. Let A_V be the anisotropy of VAMP2 peptide (all of the fluorophores are associated with VAMP2) and A_{VT} be the anisotropy of complex (all of the fluorophores are associated with the complex), then

$$A = \frac{[V]}{[V]+[VT]}A_V + \frac{[VT]}{[V]+[VT]}A_{VT} = \left(1 - \frac{[VT]}{V_0}\right)A_V + \frac{[VT]}{V_0}A_{VT}$$

thus,

$$\frac{[VT]}{V_0} = \frac{A - A_V}{A_{VT} - A_V} \tag{2}$$

Equation 1 can be written as

$$\frac{d[VT]}{dt} = k_{on}(V_0 - [VT])(T_0 - [VT]) - k_{off}[VT] \tag{3}$$

At the initial stage of the binding reaction, [VT] is close to zero. Hence, eq 3 can be simplified as

$$\frac{d[VT]}{dt} = k_{on}V_0T_0 \tag{4}$$

Combining eqs 2 and 4, we obtain

$$\frac{dA/dt}{A_{VT} - A_V} = k_{on}T_0 \tag{5}$$

To obtain k_{on}, we performed a series of reactions that labeled VAMP2 peptide binds to t-SNARE at various initial concentrations, T_0, and monitored the variation of A with t. For each T_0, we obtained the initial rate dA/dt from the A versus t curve, then plotted $(dA/dt)/(A_{VT} - A_V)$ versus T_0. The resulting data points were fitted with a simple linear regression, and the slope gave k_{on}.

When the reaction reaches equilibrium, the measured anisotropy plateaus. Let K_D be the affinity constant, A_p be the measured anisotropy at equilibrium, and $[V]_p$, $[T]_p$, and $[VT]_p$ be the concentrations of VAMP2 peptide, t-SNARE, and SNARE complex at equilibrium, respectively. Then

$$K_D = \frac{[V]_p[T]_p}{[VT]_p} = \frac{(V_0 - [VT]_p)(T_0 - [VT]_p)}{[VT]_p} \tag{6}$$

$$A_p = \left(1 - \frac{[VT]_p}{V_0}\right)A_V + \frac{[VT]_p}{V_0}A_{VT} \tag{7}$$

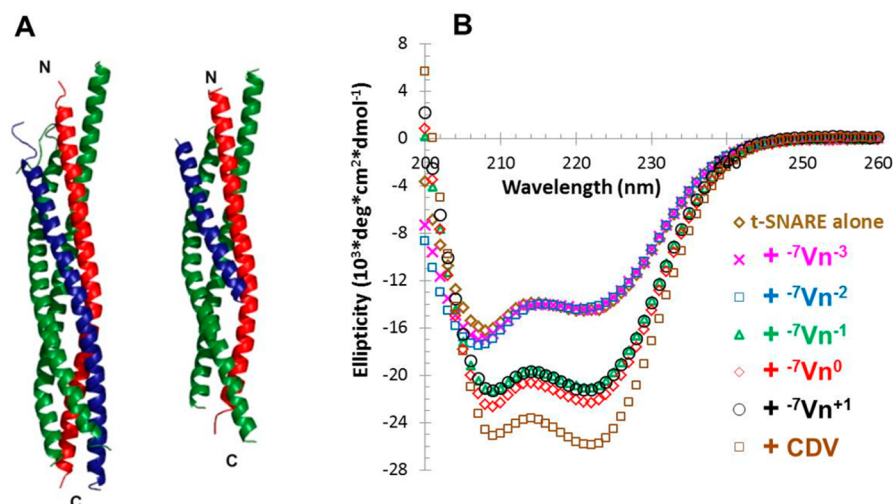Solving eq 6 for $[VT]_p$, and then entering into eq 7, we have

Figure 2. Molecular basis of the N-terminal switch. (A) Binding of $^{-7}Vn^{+1}$ prestructures the C-terminus of the t-SNARE, as seen in a comparison of the crystal structures of the postfusion SNARE complex (left) and a partially assembled complex (right). The postfusion complex exhibits four-helix structure, as four helices are present on both its N- and C-termini (synxin 1A, red; SNAP25, green; VAMP2, blue). The partially assembled SNARE complex contains a peptide $^{-7}Vn^{+1}$ binding to the t-SNARE motif, and similar to the postfusion complex, it also shows four-helix structure on both N- and C- termini, even though only three helices are present on its C-terminus. (B) Structuring of t-SNARE requires binding of $^{-7}Vn^{-1}$ or longer. t-SNARE was incubated with various Vn peptides at equimolar ratio, and their structures were monitored by circular dichroism. After incubating with $^{-7}Vn^{-1}$, $^{-7}Vn^{0}$ or $^{-7}Vn^{+1}$, respectively, the CD spectra of SNAREs became similar to postfusion SNARE complex, whereas the CD spectra of t-SNARE were not altered after incubating with $^{-7}Vn^{-2}$ and $^{-7}Vn^{-3}$, respectively.

$$A_p = A_V + (A_{VT} - A_V)$$

$$\left\{ \frac{(K_D + V_0 + T_0) - \sqrt{(K_D + V_0 + T_0)^2 - 4V_0T_0}}{2V_0} \right\} \quad (8)$$

or

$$A_p - A_V = (A_{VT} - A_V)$$

$$\left\{ \frac{(K_D + V_0 + T_0) - \sqrt{(K_D + V_0 + T_0)^2 - 4V_0T_0}}{2V_0} \right\} \quad (9)$$

By changing the initial concentration of t-SNARE, T_0, while keeping V_0 constant, one can obtain a curve of A_p as a function of T_0. K_D is obtained using eq 8 or eq 9 and applying a nonlinear regression fit to the A_p versus T_0 curve.[38]

More details about these protocols are included in the Supporting Information.

■ **RESULTS**

An NTD Assembly Induced Switch Enables CTD-LD-TMD To Drive Membrane Fusion. The model for complexin clamping is that complexin binds the half-assembled, intermediate SNARE complex and arrests further zippering and that upon clamp release, the zippering of the C-terminal portions provides sufficient energy to drive fusion (Figure 1A). To test this directly, we topologically separated NTD from later zippering reactions, thereby isolating C-terminal assembly as the only source of energy for bilayer fusion. We truncated VAMP2 at layer +1, right after the zeroth layer, generating a protein, $^{+1}Vc^{END}$, containing only CTD, LD, and TMD (VAMP2 residues from 60 to 116). $^{+1}Vc^{END}$ was reconstituted into liposomes ($^{+1}Vc^{END}$-liposomes, Supporting Information Figure S1) and nanodiscs ($^{+1}Vc^{END}$-nanodiscs). We performed two types of fusion assays. Lipid mixing of $^{+1}Vc^{END}$-liposomes or $^{+1}Vc^{END}$-nanodiscs with full length t-SNARE liposomes

(FLT-liposomes) was monitored by dequenching of membrane dye.[4] In content release assay, $CaCl_2$ that was encapsulated within FLT-liposomes was released through the fusion pores formed between FLT-liposomes and $^{+1}Vc^{END}$-nanodiscs and monitored by measuring the fluorescence of a Ca^{2+} sensor, Mag-fluo-4.[39] No specific fusion was observed (Figure 1B and Supporting Information Figure S2). However, fusion was restored when covalently separated N-terminal portion of the v-SNARE (Vn) was added. Specifically, we preincubated FLT-liposomes with $^{-7}Vn^{-1}$ peptide (the NTD region of VAMP2 from layer −7 to −1, right before the zeroth layer) and then added $^{+1}Vc^{END}$-liposomes or $^{+1}Vc^{END}$-nanodiscs to start the fusion assays (Figure 1B and Supporting Information Figure S2). The initial fusion rates of lipid mixing were ~12-fold that of the positive control, where both FLT-liposomes and FLV-liposomes (or FLV-nanodiscs) contain wild type, full length SNAREs. Interestingly, the magnitude of activation by prebound Vn is very similar to the level of activation by Munc18 (~10-fold).[26]

These results show that (i) the C-terminal (CTD-LD-TMD) assembly of SNAREs provides sufficient energy needed to drive fusion whereas the energy from the N-terminal assembly has no direct contribution to fusion and (ii) N-terminal assembly with the t-SNARE is a prerequisite to enable fusion driven by CTD-LD-TMD assembly. NTD binding switches the t-SNARE to an activated state that must be reached before fusion can occur. Therefore, the process of SNARE-mediated fusion can be functionally divided into two distinct and sequential steps, and the fusion in the positive control with full length SNAREs follows the same two-step pattern: the NTD of SNAREs assembles first and activates the t-SNARE, after which the C-termini assemble to drive fusion. The positive control is 12 times slower than the fusion between $^{+1}Vc^{END}$-liposomes and preactivated FLT-liposomes. This shows that (i) C-terminal assembly of SNAREs is rapid and not rate-limiting and that (ii)
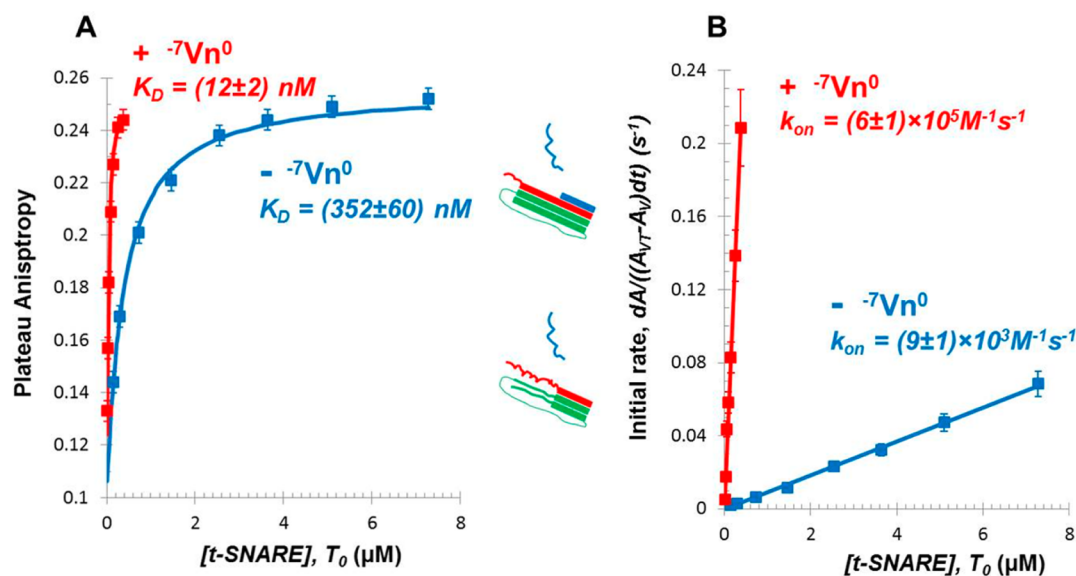
Figure 3. Structuring of the t-SNARE facilitates C-terminal assembly both energetically and kinetically. Fluorescence anisotropy experiments were performed to monitor the binding process of $^{+1}Vc^{LD}$ (VAMP2 residues 58–94) to the cytosolic t-SNARE at various concentrations with and without prebound $^{-7}Vn^0$ peptide in real time. The anisotropy versus time curves are in Supporting Information Figures S6 and S7. (A) Vn binding to the t-SNARE improves binding affinity of Vc. Plateau anisotropy values were plotted versus the concentration of t-SNARE (squares). The solid lines were fits using eq 8 in Experimental Section to obtain the affinity constants. (B) Vn binding to the t-SNARE increases the on-rate of C-terminal assembly. The initial binding rate was plotted versus the concentration of t-SNARE according to eq 5 in Experimental Section to obtain the on-rate.

the N-terminal assembly with the t-SNARE is the rate-limiting factor.

Layer −1 Is Required for the NTD Induced Switch. We further examined the ability of NTD to activate fusion for a potential length requirement for the sequence of NTD. We generated a series of NTD peptides that are truncated after the respective hydrophobic layer, ranging from $^{-7}Vn^{-4}$ (which contains VAMP2 residues from layer −7 to layer −4) to $^{-7}Vn^{+1}$ (layer −7 to +1), and tested whether they are able to activate fusion between $^{+1}Vc^{END}$-liposomes or $^{-2}Vc^{END}$-liposomes and FLT-liposomes (Figure 1C and Supporting Information Figure S3). We observed a distinct transition: Vn peptides containing layer −1 ($^{-7}Vn^{-1}$ and $^{-7}Vn^0$) both enabled fusion at similar rates, while peptides lacking layer −1 ($^{-7}Vn^{-2}$, $^{-7}Vn^{-3}$ and $^{-7}Vn^{-4}$) did not activate fusion.

Next we used fluorescence anisotropy to measure the binding between these Vn peptides and cytosolic t-SNARE. The binding curves in Figure 1D show a similar transition regarding the sequence of Vn: $^{-7}Vn^{-1}$, $^{-7}Vn^0$, and $^{-7}Vn^{+1}$ bound tightly to the t-SNARE, and the binding constants for these peptides are virtually identical (70 to 100 nM); however, $^{-7}Vn^{-2}$ and $^{-7}Vn^{-3}$ exhibited a dramatic reduction in affinity, with affinity constants of ~10 μM, showing that truncations of layer −1 of VAMP2 lead to a large loss of binding to the t-SNARE. Accordingly, we were able to reconstitute partially assembled SNARE complexes from syntaxin 1A, SNAP25, and $^{-7}Vn^{-1}$ or longer but not with $^{-7}Vn^{-2}$, as assessed by gel filtration analysis (Supporting Information Figure S4). We observe an all-or-nothing transition, revealing a binary switch on the N-terminus of SNAREs, with the minimum sequence being layer −7 to layer −1 (Figure 1C and Figure 1D). Only upon the binding of $^{-7}Vn^{-1}$ or longer versions is the t-SNARE switched "on" for fusion.

NTD Assembly Activates Fusion by Prestructuring the t-SNARE. To investigate the molecular basis for the N-terminal activation, we compared the crystal structures of a postfusion,

fully zippered SNARE complex[8,16] and a partially assembled, half-zippered complex.[34] The fully assembled complex displays a four-helix bundle structure from N- to C-termini, as there are four helices present on both N- and C-termini. The partially assembled SNARE complex mimicked an intermediate folding state with a Vn peptide, $^{-7}Vn^{+1}$, which was reconstituted into a complex with the complete t-SNARE motifs. The crystal structure of the resulting half-zippered SNARE complex ($^{-7}SNARE^{+1}$) showed that surprisingly the SNARE motifs of syntaxin and SNAP25 almost entirely adopt an α-helical conformation (Figure 2A): even though the C-terminal half of the complex only consists of three helices, they still display exactly the same four-helix bundle configuration as in the fully zippered complex. Previous studies have shown that the binary syntaxin/SNAP25 t-SNARE complex is unstructured in its C-terminal portion,[18,40,41] implying together with our data that binding of VAMP2 NTD to the t-SNARE triggers a binary switch that propagates the four-helix bundle geometry to the t-SNARE C-terminal domain.

To confirm this by an independent method, we next tested if the Vn peptides that enable fusion mediated by membrane attached Vc are capable of structuring the t-SNARE in solution. The transition from the partially unstructured t-SNARE to the folded SNARE core complex can be monitored using circular dichroism (CD) where the higher helical content of the ternary complex leads to a strong increase in ellipticity (Figure 2B). All Vn peptides that activate fusion do in fact induce helical structure. Importantly, the truncated SNARE complex adopts a state of intermediate folding/helicity more similar to the SNARE core than the t-SNARE. This shows that the structure observed in the crystal is a true representation of the solution structure. The increase in ellipticity for $^{-7}Vn^{-1}$ and $^{-7}Vn^0$ is similar to that of $^{-7}Vn^{+1}$, suggesting the formation of a similar structure. In contrast, $^{-7}Vn^{-2}$ and $^{-7}Vn^{-3}$, which do not activate fusion, have no effect on t-SNARE conformation when they were added at equimolar ratio or 5-fold molar excess (Figure
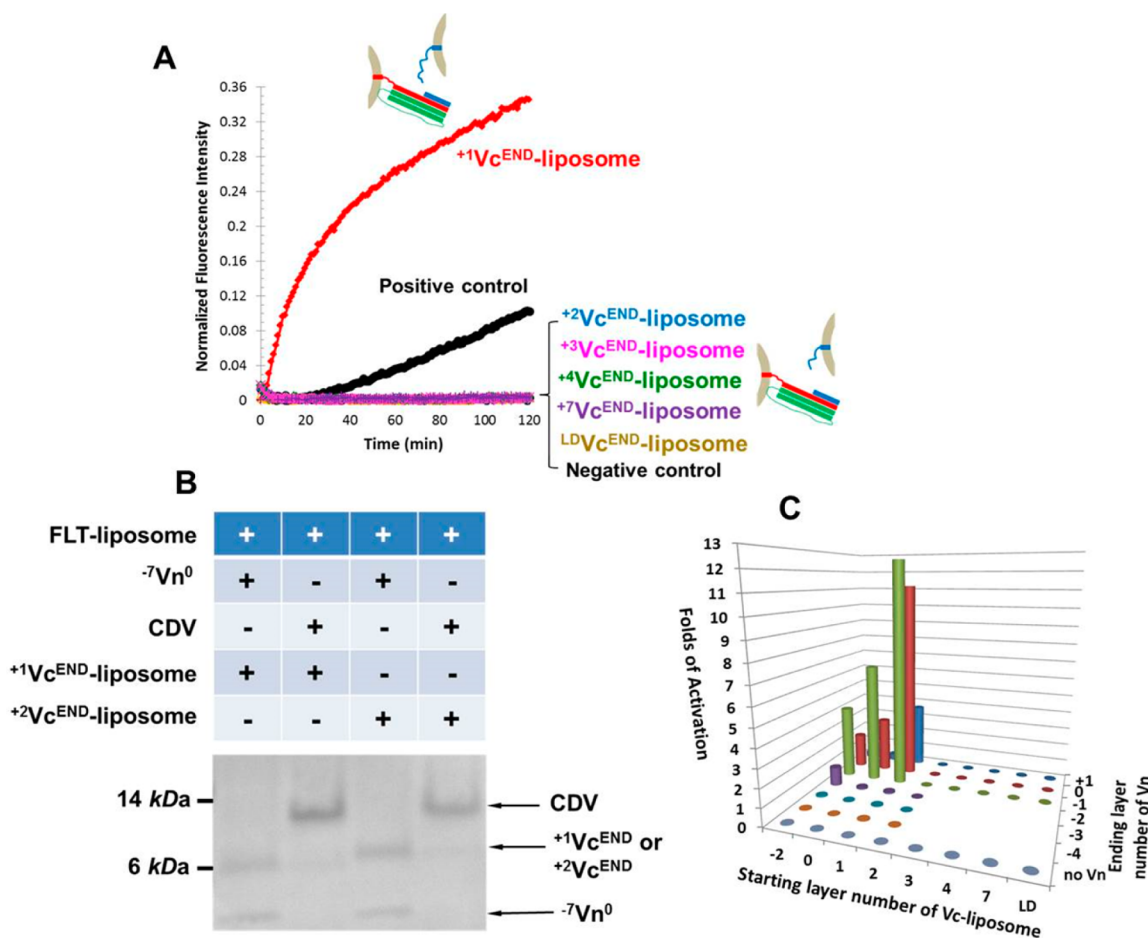
Figure 4. The C-termini of SNAREs are required to assemble from layer +1 to their end to drive membrane merging. (A) Fusion assay between FLT-liposomes with prebound $^{-7}Vn^{-1}$ and various Vc-liposomes: $^{+1}Vc^{END}$-liposome, $^{+2}Vc^{END}$-liposome, $^{+3}Vc^{END}$-liposome, $^{+4}Vc^{END}$-liposome, $^{+7}Vc^{END}$-liposome, $^{LD}Vc^{END}$-liposome, respectively. A sharp transition was observed between layers +1 and +2. In the absence of layer +1, Vc-liposomes lost their capability to drive fusion. (B) $^{+1}Vc^{END}$-liposomes and $^{+2}Vc^{END}$-liposomes were able to dock to FLT-liposomes. In a His-tag pull-down, FLT-liposomes were first incubated with $^{-7}Vn^0$ or CDV at 37 °C for 1 h, followed by incubation with various Vc-liposomes at 37 °C for 2 h, then pulled down by nickel-NTA through the His-tag on SNAP25. Undocked Vc-liposomes were washed away. The final products were analyzed by SDS−PAGE. (C) A map of fusion activation that illustrates the sequence requirements for both N- and C-termini. Data for this plot and errors of measurements are in Supporting Information Table S2.

2B). As a concentration-independent measure of helical content, the ratio of ellipticity at 222 and 208 nm can be compared (Supporting Information Figure S5). This result follows the same length requirement as the fusion assay and binding assay for different lengths of Vn peptides.

Taken together, our observations show that activation of fusion, peptide binding, and induction of helicity are all coupled in an all-or-nothing transition, revealing that the molecular basis of this binary switch is the structuring of the C-terminal domain of the t-SNARE. Specifically, binding of Vn induces the three helices of the t-SNARE CTD to adopt the same configuration as in the fully assembled, postfusion complex, resulting in a preformed binding site for the fourth helix, the C-terminal domain of VAMP2.

Prestructuring of the t-SNARE Facilitates CTD-LD Assembly Both Energetically and Kinetically. The N-terminal activation of the SNAREs profoundly impacts the assembly and fusion on their C-termini. To accurately quantify this effect, we used fluorescence anisotropy measurements and monitored the rate of assembly of a soluble Vc peptide, $^{+1}Vc^{LD}$ (which includes VAMP2 residues 58−94, layers +1 to +8 plus linker domain), with soluble, cytosolic portion of the t-SNARE

in the presence and absence of $^{-7}Vn^0$ in real time (Figure 3A and Figure 3B, Supporting Information Figures S6 and S7). In the absence of $^{-7}Vn^0$, rate of binding of Vc to the t-SNARE is slow ($k_{on} = (9 \pm 1) \times 10^3 M^{-1} s^{-1}$) and thermodynamically less favorable ($K_D = 352 \pm 60$ nM), which corresponds to a free energy of $-14.9 \pm 0.2 k_BT$, where k_B is the Boltzmann constant. When the t-SNARE was switched on upon binding Vn, the kinetics of C-terminal domain assembly was increased ∼70 times (now $k_{on} = (6 \pm 1) \times 10^5 M^{-1} s^{-1}$) and affinity of Vc was increased by ∼30-fold to $K_D = 12 \pm 2$ nM, corresponding to a free energy $-18.3 \pm 0.2 k_BT$. As shown above, the energy that overcomes the fusion barrier comes from the assembly of C-terminus (layer +1 to layer +8 plus linker domain). This suggests that an extra free energy of $-3.4 k_BT$ is generated when t-SNARE is in the "on" state and that this additional energy is required for rapid fusion to occur.

The on-rate of Vc assembling with preactivated t-SNARE is also rapid, with $k_{on} = (6 \pm 1) \times 10^5 M^{-1} s^{-1}$. Considering the concentration of SNAREs between two docked membranes is ∼1 mM,[34] the on-rate becomes ∼$10^3 s^{-1}$ (time constant of ∼1 ms), which is very close to the rate measured by optical tweezers.[20] This kinetics is of the same order of magnitude as

the submillisecond scale kinetics of synaptic vesicle measured by electrophysiology studies.[42−44] Furthermore, Vc was separated from Vn in our experimental design. What we measured was an intermolecular binding, and this underestimated the real kinetics. Under physiological conditions, Vc and Vn are located within a single molecule, and after Vn prebinds the t-SNARE, C-terminal assembly will be an intramolecular binding, making the local concentration of Vc even higher (probably ∼0.1 M), and thus, the reaction will be even faster than the kinetics we measured here. Hence the rapid C-terminal assembly of the SNAREs should be capable of driving fusion at the time scale required in synaptic vesicle fusion. Therefore, structuring of the t-SNARE C-terminal domain accelerates assembly of Vc both energetically and kinetically by lowering the entropy of the t-SNARE as well the activation barrier of assembly, which is the mechanism underlying activation of fusion.

Layer +1 Is Required for CTD-LD Assembly To Trigger Fusion. We also examined the length requirements of the liposome-attached Vc by systematically testing a series of Vc-liposomes (Supporting Information Figure S1) in the fusion assay using FLT-liposomes. When the FLT-liposomes were not preincubated with Vn, no specific fusion occurred for all these Vc constructs (Supporting Information Figure S8). When the t-SNAREs were preassembled with $^{-7}Vn^{-1}$ (Figure 4A, Supporting Information Figures S9) or with $^{-7}Vn^{0}$ (Supporting Information Figures S10 and S11) to make sure that the t-SNARE was in the "on" state, the fusion capability of these Vc-liposomes also exhibited an all-or-nothing behavior. All Vc-liposomes containing layer +1 ($^{+1}Vc^{END}$-liposomes or longer) fused with prestructured FLT-liposomes with an elevated rate, while all Vc-liposomes lacking layer +1 ($^{+2}Vc^{END}$-liposomes or shorter) did not fuse with prestructured FLT-liposomes. Fusion results between FLT-liposomes and Vc-nanodiscs showed similar transition between layers +1 and +2 (Supporting Information Figure S12). This shows that (i) the CTD-LD-TMD assembly that triggers fusion also behaves as a binary switch and (ii) layer +1 has a critical role in fusion, without which fusion is completely abolished.

Two factors may be responsible for fusion incompetency of $^{+2}Vc^{END}$-liposomes or shorter: (i) a docking defect which means that $^{+2}Vc^{END}$-liposomes or shorter do not bind prestructured FLT-liposomes; (ii) fusion defect, where the energy obtained from zippering layer +1 to TMD is just enough to overcome the energy barriers of C-terminal assembly and fusion, while zippering from layer +2 to TMD does not provide enough energy. To determine which the dominant factor is, we performed a His-tag pull-down assay (Figure 4B). Vc-liposomes contained no His-tag, while FLT-liposomes were His-tagged. Vc-liposomes were only pulled down when they docked on FLT-liposomes. SDS−PAGE analysis showed that the fusion-potent construct, $^{+1}Vc^{END}$-liposomes, and the fusion-incompetent construct, $^{+2}Vc^{END}$-liposomes, could both dock to FLT-liposomes. Even though the pull-down experiment cannot prove that docking is quantitatively the same, this result suggests that fusion incompetency of $^{+2}Vc^{END}$-liposomes or shorter versions was most likely due to their inability to generate sufficient energy required for C-terminal assembly and fusion.

By systematically testing the sequence requirements for N-terminal activation and C-terminal fusion, we are able to generate a comprehensive map of fusion activation (Figure 4C). The optimal combination is that FLT-liposome is

activated by $^{-7}Vn^{-1}$ and then fuses with $^{+1}Vc^{END}$-liposome. Compared with the standard FLV-liposome/FLT-liposome fusion reaction, this pair results in ∼12-fold activation.

■ DISCUSSION

Membrane fusion ultimately requires the assembly of t- and v-SNAREs into a four-helix bundle which brings the membranes into close proximity and triggers bilayer merging. Formation of cis-SNARE complex was proposed to occur through continuous and progressive zippering from N-termini to C-termini and to culminate in a release of energy to drive membrane fusion.[13−15] Our data show that functionally, a two-step sequential zippering pathway is required in membrane fusion, and each step has its specific and distinct function (Figure 5). In both steps,
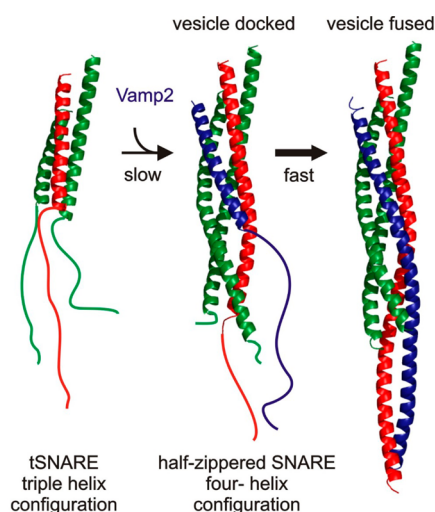

Figure 5. Fusion model. Membrane merging is driven by the two-step SNARE assembly pathway. First the N-termini of SNAREs assemble to at least layer −1 and switch the t-SNARE into fusion-ready conformation (docking and structuring). Then the C-termini of SNAREs assemble (starting at least from layer +1) and provide energy to overcome the fusion barrier. The docking and structuring step is the rate-limiting step.

zippering exhibits all-or-nothing, binary-switch-like behavior. The first step is characterized by docking and t-SNARE structuring and requires t- and v-SNAREs to zipper to at least layer −1 (assembly of layer −7 to layer −2 or shorter can barely dock the v-SNARE to the t-SNARE because binding of $^{-7}Vn^{-2}$ or shorter versions to the t-SNARE is extremely weak, with affinities ∼10 μM). The long-range effect of Vn binding on the structure of the t-SNARE C-terminus can best be explained by an "induced-fit" conformational transition of the t-SNARE from a triple-helix to a four-helix bundle configuration. The second step defines actual fusion, where t- and v-SNAREs assemble from layer +1 to the transmembrane domain and energy generated from this step of zippering is used to overcome the fusion barrier. These findings are intrinsic properties of the SNAREs; in vivo, regulatory proteins such as synaptotagmin may help stalk formation and pore opening. Whereas the fusion step occurs very rapidly, the docking and structuring step is rate-limiting for membrane fusion. Our data suggest that the ionic layer, layer 0, does not have a functional role in either of the two assembly steps. However, it is possible that it separates NTD and CTD-LD-TMD from each other.

In the conventional N-to-C zippering model, the very N-termini of the SNAREs have been presumed as the point where the assembly process is initiated.[17] Here we show that N-terminal assembly has to reach the middles layers (around layer −1) to induce a dramatic transition that (i) achieves a much higher binding affinity than that in the N-terminal layers, (ii) introduces a significant structural change in the t-SNARE, and (iii) facilitates C-terminal zippering of the SNARE complex. These data suggest that the middle layers are the critical part for assembly of the entire SNAREpin.

Previously, a soluble Vc peptide (VAMP2 residues 57−92) was found to accelerate fusion between FLT-liposomes and FLV-liposomes.[13,14] Melia et al. proposed a molecular mechanism for this finding,[13] suggesting that binding of Vc to the t-SNARE displaced the N-terminal regulatory domain of syntaxin and opened up the t-SNARE. However, in the current view of the folding pathway of the SNAREs, because of the topological constraints, the N-termini zipper first, then followed by C-terminal assembly. Here we use Vn peptides to prebind the t-SNARE and liposome-reconstituted Vc to initiate fusion. This design perfectly matches the folding pathway of the SNAREs because it is completely viable that physiologically full length VAMP2 uses its N-terminal portion to bind and prestructure the t-SNARE and then further zippers up its C-terminal portion with the t-SNARE to drive fusion. Hence, activation of fusion by Vn, but probably not Vc, is likely to be relevant under physiological conditions.

Other groups reported that Vn peptides that contained layers −7 to 0 (or longer) inhibited assembly and fusion of full length SNAREs.[13,14] In our experiments, when FLT-liposomes were prebound with $^{-7}Vn^0$ (Supporting Information Figure S10), the rate of fusion with FLV-liposomes was about half the rate of the positive control (fusion between FLT-liposomes and FLV-liposomes in the absence of Vn), the result was inhibition, which is consistent with these reports.[13,14] However, when FLT-liposomes were prebound with $^{-7}Vn^{-1}$ (Supporting Information Figure S9), the rate of fusion with FLV-liposomes was about twice the rate of the positive control, the result was activation. There are two factors affecting the fusion rate: (i) prestructuring of the t-SNARE and (ii) overlap of residues between Vn peptide and FLV-liposomes. Such overlap decreases the efficiency of collision and thus decreases fusion rate in a systematic manner. The overall effect is a combination of these factors. If FLT-liposomes were prebound with $^{-7}Vn^{-1}$, prestructuring was the dominant factor and the result was activation; however, if FLT-liposomes were prebound with $^{-7}Vn^0$ or longer, more residues overlapped and this factor overcame the prestructuring, and the overall result was inhibition. Supporting Information Table S2 summarizes the various rates we measured.

The significance of the two-step assembly pathway becomes apparent in the context of regulatory proteins that influence fusion rates. Complexin has been suggested to promote t- and v-SNARE interaction by binding with its central domain to a groove formed by VAMP2 and syntaxin,[23,34,45] while its accessory domain binds the t-SNARE to block progression of fusion.[33,34] The N-terminal switch allows recruiting complexin and creation of a clamped state, as both interactions occur with the half-zippered SNARE complex. The three aspartic acid residues, which are required by Ca^{2+}-dependent removal of the clamp,[46] are located on the CTD of VAMP2 (between layers +2 and +4). As soon as the SNAREs zipper to around layer +1 or +2, complexin switches to the closed conformation simultaneously. A further physiologically meaningful intermediate pause in the SNARE folding pathway cannot exist after the action of complexin switch occurs, which indicates that the C-terminal zippering of the SNAREs may happen as a single event. This is consistent with our finding that assembly of $^{+2}Vc^{END}$ or shorter versions with the prestructured t-SNARE is not capable of driving fusion. These results suggest that it is unlikely that there is another relevant intermediate state in the C-terminal assembly step of the SNAREs. The two-step assembly becomes both kinetically and thermodynamically observable in the presence of complexin.[23] Therefore, this switchlike, two-step folding pathway plays a critical role under physiological conditions and the half-zippered SNARE complex represents a previously unrecognized important intermediate stage of the SNARE assembly.

■ ASSOCIATED CONTENT

Ⓢ Supporting Information
Figures S1−S12, Tables S1 and S2, and Materials and Methods with detailed description of materials, protein constructs and purifications, and protocols of the assays used in this study. This material is available free of charge via the Internet at http://pubs.acs.org.

■ AUTHOR INFORMATION

Corresponding Authors
feng.li@yale.edu
pincet@lps.ens.fr

Present Address
§D.K.: Universität Osnabrück, Barbarastrasse 13, 67/E44, 49076 Osnabrück, Germany.

Notes
The authors declare no competing financial interest.

■ ACKNOWLEDGMENTS

■ REFERENCES

(1) Sollner, T.; Whiteheart, S. W.; Brunner, M.; Erdjument-Bromage, H.; Geromanos, S.; Tempst, P.; Rothman, J. E. *Nature* **1993**, *362*, 318.
(2) Sudhof, T. C.; Rothman, J. E. *Science* **2009**, *323*, 474.
(3) Hu, C.; Ahmed, M.; Melia, T. J.; Sollner, T. H.; Mayer, T.; Rothman, J. E. *Science* **2003**, *300*, 1745.
(4) Weber, T.; Zemelman, B. V.; McNew, J. A.; Westermann, B.; Gmachl, M.; Parlati, F.; Sollner, T. H.; Rothman, J. E. *Cell* **1998**, *92*, 759.
(5) Brunger, A. T. *Q. Rev. Biophys.* **2005**, *38*, 1.
(6) Rizo, J.; Rosenmund, C. *Nat. Struct. Mol. Biol.* **2008**, *15*, 665.
(7) Sollner, T.; Bennett, M. K.; Whiteheart, S. W.; Scheller, R. H.; Rothman, J. E. *Cell* **1993**, *75*, 409.
(8) Sutton, R. B.; Fasshauer, D.; Jahn, R.; Brunger, A. T. *Nature* **1998**, *395*, 347.
(9) Fasshauer, D.; Sutton, R. B.; Brunger, A. T.; Jahn, R. *Proc. Natl. Acad. Sci. U.S.A.* **1998**, *95*, 15781.
(10) Fasshauer, D.; Otto, H.; Eliason, W. K.; Jahn, R.; Brunger, A. T. *J. Biol. Chem.* **1997**, *272*, 28036.
(11) Margittai, M.; Fasshauer, D.; Pabst, S.; Jahn, R.; Langen, R. *J. Biol. Chem.* **2001**, *276*, 13169.

(12) Hanson, P. I.; Roth, R.; Morisaki, H.; Jahn, R.; Heuser, J. E. *Cell* **1997**, *90*, 523.

(13) Melia, T. J.; Weber, T.; McNew, J. A.; Fisher, L. E.; Johnston, R. J.; Parlati, F.; Mahal, L. K.; Sollner, T. H.; Rothman, J. E. *J. Cell Biol.* **2002**, *158*, 929.

(14) Pobbati, A. V.; Stein, A.; Fasshauer, D. *Science* **2006**, *313*, 673.

(15) Li, F.; Pincet, F.; Perez, E.; Eng, W. S.; Melia, T. J.; Rothman, J. E.; Tareste, D. *Nat. Struct. Mol. Biol.* **2007**, *14*, 890.

(16) Stein, A.; Weber, G.; Wahl, M. C.; Jahn, R. *Nature* **2009**, *460*, 525.

(17) Jahn, R.; Fasshauer, D. *Nature* **2012**, *490*, 201.

(18) Fiebig, K. M.; Rice, L. M.; Pollock, E.; Brunger, A. T. *Nat. Struct. Biol.* **1999**, *6*, 117.

(19) Sorensen, J. B.; Wiederhold, K.; Muller, E. M.; Milosevic, I.; Nagy, G.; de Groot, B. L.; Grubmuller, H.; Fasshauer, D. *EMBO J.* **2006**, *25*, 955.

(20) Gao, Y.; Zorman, S.; Gundersen, G.; Xi, Z.; Ma, L.; Sirinakis, G.; Rothman, J. E.; Zhang, Y. *Science* **2012**, *337*, 1340.

(21) Sørensen, J. B. *Annu. Rev. Cell Dev. Biol.* **2009**, *25*, 513.

(22) Weber, J. P.; Reim, K.; Sorensen, J. B. *EMBO J.* **2010**, *29*, 2477.

(23) Li, F.; Pincet, F.; Perez, E.; Giraudo, C. G.; Tareste, D.; Rothman, J. E. *Nat. Struct. Mol. Biol.* **2011**, *18*, 941.

(24) Hata, Y.; Slaughter, C. A.; Sudhof, T. C. *Nature* **1993**, *366*, 347.

(25) Verhage, M.; Maia, A. S.; Plomp, J. J.; Brussaard, A. B.; Heeroma, J. H.; Vermeer, H.; Toonen, R. F.; Hammer, R. E.; van den Berg, T. K.; Missler, M.; Geuze, H. J.; Sudhof, T. C. *Science* **2000**, *287*, 864.

(26) Shen, J.; Tareste, D. C.; Paumet, F.; Rothman, J. E.; Melia, T. J. *Cell* **2007**, *128*, 183.

(27) Weninger, K. R. *Nat. Struct. Mol. Biol.* **2011**, *18*, 861.

(28) Fernandez-Chacon, R.; Konigstorfer, A.; Gerber, S. H.; Garcia, J.; Matos, M. F.; Stevens, C. F.; Brose, N.; Rizo, J.; Rosenmund, C.; Sudhof, T. C. *Nature* **2001**, *410*, 41.

(29) Reim, K.; Mansour, M.; Varoqueaux, F.; McMahon, H. T.; Sudhof, T. C.; Brose, N.; Rosenmund, C. *Cell* **2001**, *104*, 71.

(30) Giraudo, C. G.; Eng, W. S.; Melia, T. J.; Rothman, J. E. *Science* **2006**, *313*, 676.

(31) Melia, T. J., Jr. *FEBS Lett.* **2007**, *581*, 2131.

(32) Malsam, J.; Parisotto, D.; Bharat, T. A.; Scheutzow, A.; Krause, J. M.; Briggs, J. A.; Sollner, T. H. *EMBO J.* **2012**, *31*, 3270.

(33) Giraudo, C. G.; Garcia-Diaz, A.; Eng, W. S.; Chen, Y.; Hendrickson, W. A.; Melia, T. J.; Rothman, J. E. *Science* **2009**, *323*, 512.

(34) Kummel, D.; Krishnakumar, S. S.; Radoff, D. T.; Li, F.; Giraudo, C. G.; Pincet, F.; Rothman, J. E.; Reinisch, K. M. *Nat. Struct. Mol. Biol.* **2011**, *18*, 927.

(35) Parlati, F.; Weber, T.; McNew, J. A.; Westermann, B.; Sollner, T. H.; Rothman, J. E. *Proc. Natl. Acad. Sci. U.S.A.* **1999**, *96*, 12565.

(36) Ji, H.; Coleman, J.; Yang, R.; Melia, T. J.; Rothman, J. E.; Tareste, D. *Biophys. J.* **2010**, *99*, 553.

(37) McNew, J. A.; Weber, T.; Parlati, F.; Johnston, R. J.; Melia, T. J.; Sollner, T. H.; Rothman, J. E. *J. Cell Biol.* **2000**, *150*, 105.

(38) Heyduk, T.; Lee, J. C. *Proc. Natl. Acad. Sci. U.S.A.* **1990**, *87*, 1744.

(39) Shi, L.; Shen, Q. T.; Kiel, A.; Wang, J.; Wang, H. W.; Melia, T. J.; Rothman, J. E.; Pincet, F. *Science* **2012**, *335*, 1355.

(40) Fasshauer, D.; Margittai, M. *J. Biol. Chem.* **2004**, *279*, 7613.

(41) Munson, M.; Hughson, F. M. *J. Biol. Chem.* **2002**, *277*, 9375.

(42) Sun, J.; Pang, Z. P.; Qin, D.; Fahim, A. T.; Adachi, R.; Sudhof, T. C. *Nature* **2007**, *450*, 676.

(43) Wolfel, M.; Schneggenburger, R. *J. Neurosci.* **2003**, *23*, 7059.

(44) Sabatini, B. L.; Regehr, W. G. *Nature* **1996**, *384*, 170.

(45) Chen, X.; Tomchick, D. R.; Kovrigin, E.; Arac, D.; Machius, M.; Sudhof, T. C.; Rizo, J. *Neuron* **2002**, *33*, 397.

(46) Krishnakumar, S. S.; Radoff, D. T.; Kummel, D.; Giraudo, C. G.; Li, F.; Khandan, L.; Baguley, S. W.; Coleman, J.; Reinisch, K. M.; Pincet, F.; Rothman, J. E. *Nat. Struct. Mol. Biol.* **2011**, *18*, 934.

3464

dx.doi.org/10.1021/ja410690m | *J. Am. Chem. Soc.* 2014, 136, 3456−3464